A metrological approach for the calibration of force transducers with interferometric readout

Surface Topography: Metrology and Properties

PAPER

A metrological approach for the calibration of force transducers with interferometric readout

S V Beekmans and D Iannuzzi

Department of Physics and Astronomy and LaserLab Amsterdam, VU University, Amsterdam, The Netherlands

E-mail: s.v.beekmans@vu.nl

Abstract

We introduce an experimental calibration method for force transducers with interferometric readout. The head of the transducer is compressed on the pan of a weighing scale until the first maximum of interference is reached. An optomechanical feedback loop makes sure that the force applied remains constant during the integration time of the weighing scale. At the end of the integration time, the transducer is forced to move to the next maximum of interference, where it is again locked into position to allow the user to read the corresponding increase in weight on the scale. Repeating a similar procedure for a series of consecutive maximum-to-maximum steps, one can finally plot the weight indicated by the scale as a function of the displacement of the head of the transducer, and, from there, extract its spring constant. The method relies only on measurements of weights and laser wavelengths, both of which can be, in principle, referred to metrological standards.

1. Introduction

Micro- and nanomachined linear force transducers often rely on two main components: a spring that bends in proportion to the force applied to the sensing head, and a readout unit that measures the extent of that bending. To translate the output of the readout unit into force, one needs to know the spring constant of the spring, which has thus to be accurately calibrated [1, 2]. Unfortunately, calibration is not always a straightforward procedure. In the field of atomic force microscopy (AFM), for instance, despite the numerous calibration methods already developed to assess the spring constant of cantilevers (for an overview see [3]), there is still no accepted protocol that can provide accurate values in all circumstances. Dynamic calibration methods, in fact, make use of mechanical models and simulations that may hinge on heavy approximations [4–9] and that may require accurate knowledge of the geometrical features of the spring [3, 10–15]. Static calibration procedures, on the contrary, can provide direct accurate measurements [8, 16–18], but often necessitate tedious steps and extensive know-how to be correctly implemented.

To solve this problem, Doering *et al* proposed an alternative static method that can be implemented via

a series of straightforward steps [19]. The method relies on the idea of mounting the AFM cantilever on a calibrated piezoelectric translation stage, which is then used to push the free handing end of the cantilever against the pan of a weighing scale. The spring constant of the cantilever is inferred by measuring the weight indicated by the scale as a function of the extension of the piezoelectric device, which is assumed to be equal to the bending of the cantilever. Despite its simplicity, this approach seems to have the potential to outperform all the other static methods proposed so far in the literature [19]. However, the method suffers from a few limitations. In first place, one needs to rely on the calibration of the piezoelectric translator—an assumption that may affect the systematic error of the measurement. Furthermore, during the integration time that the weighing scale needs to measure the force applied, the bending of the cantilever must be kept constant—a technical detail that may become quite detrimental in the presence of vibrations, especially for a long integration time. Finally, because of the rather long mechanical loop of the setup (several centimeters), the system may suffer from long term drifts, which may again give rise to significant errors.

In this paper, we show that, for a force transducer equipped with interferometric readout (such as those
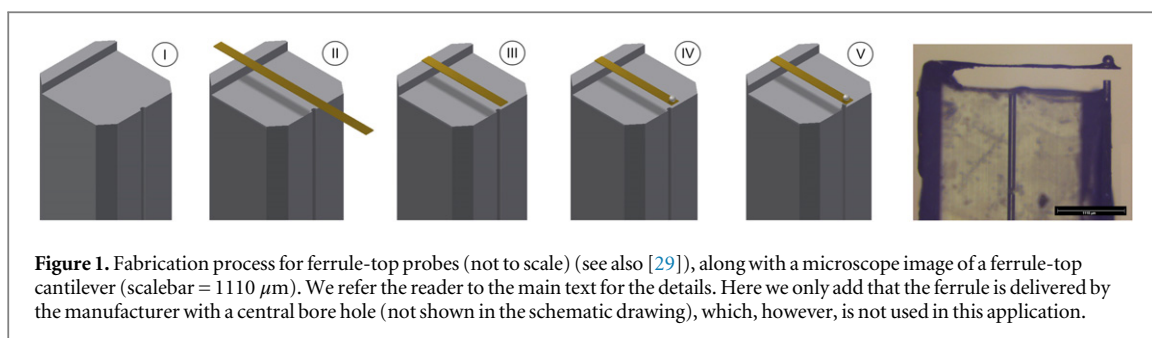
Figure 1. Fabrication process for ferrule-top probes (not to scale) (see also [29]), along with a microscope image of a ferrule-top cantilever (scalebar = 1110 μm). We refer the reader to the main text for the details. Here we only add that the ferrule is delivered by the manufacturer with a central bore hole (not shown in the schematic drawing), which, however, is not used in this application.
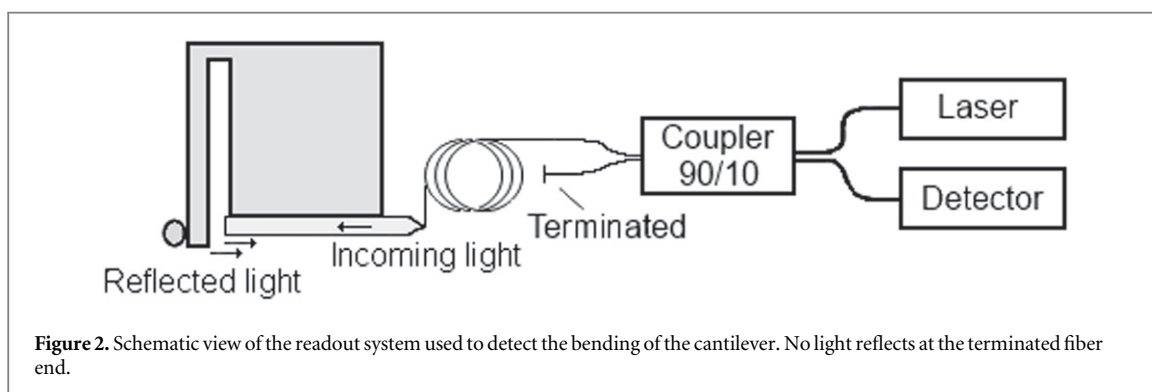

Figure 2. Schematic view of the readout system used to detect the bending of the cantilever. No light reflects at the terminated fiber end.

proposed, for instance, in [20–23]), one can refine the weighing scale method by adding a high gain negative feedback loop designed to keep the bending of the cantilever equal to a multiple of the wavelength of the readout laser. The method relies only on measurements of weights and laser wavelengths, both of which can be referred, in principle, to metrological standards. To demonstrate the feasibility of our approach, we present the results obtained while testing it on a ferrule-top micromachined device [24–26], which has already been proven to be an interesting candidate for the development of a new generation of AFMs [27–29].

2. Experimental details

2.1. Ferrule-top cantilevers: fabrication

The ferrule-top transducer used in our experiment is obtained by gluing a borosilicate cantilever on top of a borosilicate ferrule. The position of the free-hanging end of the cantilever can be monitored via a single mode optical fiber, anchored to the side of the ferrule. The most important steps of the fabrication process are shown in figure 1 (see also [29]).

In step I, a $3 \times 3 \times 7$ mm^3 borosilicate ferrule is mounted on a wire cutter to carve a $3 \times 0.4 \times 0.4$ mm^3 ridge on the top facet of the ferrule and a groove with a cross section of 0.2×0.4 mm^2 on the side opposite to the ridge. The ferrule is then taken out of the wire cutter and positioned under a microscope equipped with micrometer precision manipulators. In step II, a borosilicate cantilever, previously coated with chromium (10 nm) and gold (100 nm), is

aligned with the groove and glued with wax onto the ridge[1]. In step III, the ferrule is mounted on a ps-laser ablation system (Optec System with Lumera Laser source) to cut the cantilever on both ends of the ferrule. Because of the high accuracy of the ablation process the length of the cantilever can be very precisely determined (5 μm resolution). In step IV, a glass sphere (radius equal to 100–150 μm) is glued at the tip of the cantilever. Finally, in step V, a cleaved single mode optical fiber (Corning SMF28) is slid and glued into the lateral groove. This fiber will be used to detect the deflection of the cantilever, as explained in section 2.2. The ferrule, the cantilever and the fiber are so well held together by the wax and the glue that the sensor can be treated as a single mechanical piece. Using this method we have prepared a macro cantilever with length (L) equal to 2.65 mm, width (w) equal to 0.16 mm, and thickness (t) equal to 0.02 mm[2] (see figure 1).

2.2. Ferrule-top cantilevers: readout

The detection of cantilever bending relies on Fabry-Pérot interferometry and has been described in previous papers [20, 23, 24]. The distal end of the readout fiber is connected to a laser via an optical fiber coupler, as

---

[1] The wax dries to a very hard material that adheres well to both the ferrule and the cantilever. Drift and stress tests in ambient environment showed no observable difference between wax and various epoxy glues.

[2] Although the size of this cantilever differs significantly from standard AFM cantilevers, the method illustrated in this paper holds for cantilevers of any size or stiffness, as long as there is no significant mechanical drift between the position of the end of the fiber and that of the cantilever.

illustrated in figure 2. At the cleaved end of the fiber, a small part of the incident laser light reflects back. Most of the light, however, passes through the end and reflects on the metal interface underneath the cantilever. The two signals (i.e., the one reflected at the cleaved end of the fiber and the one reflected by the cantilever bottom surface) create an interference pattern whose amplitude is measured via a photodiode aligned with the exit of the coupler. Following [20, 24], if multiple reflections are neglected, one can describe the amplitude of the ideal interference signal in the photodiode by[3]:

$$W(d) = W_0 \left[1 + V \cos\left(\frac{4\pi d}{\lambda} + \varphi_0 \right) \right], \quad (1)$$

where d is the gap size, φ_0 is a constant phase shift that only depends on the geometry of the probe, λ is the wavelength of the laser, and W_0 and V are the midpoint interference signal and the fringe visibility, respectively. Movement of the cantilever causes a change in the size of the gap between the cantilever and the fiber end. This, in turn, leads to a change in the interference signal. By monitoring this signal, one can measure cantilever displacements.

2.3. Calibration method: overview

The calibration method presented in this paper relies on the idea to push the free hanging end of the cantilever against a calibrated weighing scale, measure the weight registered by the balance as a function of the cantilever deflection, and use Hooke's law [30] to extract the spring constant of the cantilever from the weight registered by the scale and the wavelength of the laser used in the readout.

To achieve this goal, the wavelength of the laser is modulated around a fixed value λ_0 according to:

$$\lambda(t) = \lambda_0 + \delta\lambda \cos(\omega t), \quad (2)$$

where $\delta\lambda$ and ω represent the amplitude and the angular frequency of the oscillation, respectively. Substituting equation (2) in equation (1), one obtains the expected time dependent function of the readout output:

$$W(t) \propto \cos\left[\frac{4\pi d}{\lambda_0 + \delta\lambda \cos(\omega t)} + \varphi_0 \right]$$
$$= \cos\left[\frac{\alpha}{1+x} + \varphi_0 \right], \quad (3)$$

where

$$\alpha = \frac{4\pi d}{\lambda_0} \quad (4)$$

and

$$x = \frac{\delta\lambda \cos(\omega t)}{\lambda_0} \quad (5)$$

[3] Mode hopping in the laser is minimized by introducing an isolator in the optical path.

For small values of $\delta\lambda/\lambda_0$, equation (4) can be approximated by the first order Taylor expansion around $x = 0$:

$$W(x) \propto \cos\left(\alpha + \varphi_0 \right) + \alpha \sin\left(\alpha + \varphi_0 \right)$$
$$\times x + O\left(x^2 \right). \quad (6)$$

Let us assume that the cantilever is compressed against the pan of the balance of an amount d_1 such that:

$$\alpha + \varphi_0 = \frac{4\pi d_1}{\lambda_0} + \varphi_0$$
$$= \frac{1}{2} \pi \times n, \quad n = 1, 3, 5, \dots \quad (7)$$

which implies that, for $\lambda = \lambda_0$, the output signal of the readout is at quadrature. Under these circumstances, as the wavelength of the laser oscillates around λ_0, the readout signal contains a component that oscillates at frequency ω:

$$W(t) \propto 0 + \left[\frac{4\pi d}{\lambda_0} \right]$$
$$\times \frac{\delta\lambda}{\lambda_0} \cos(\omega t) + O\left(x^2 \right). \quad (8)$$

Now let us assume that the cantilever is compressed against the pan of the balance of an amount d_2 such that:

$$\alpha + \varphi_0 = \frac{4\pi d_2}{\lambda_0} + \varphi_0 = 2\pi \times n,$$
$$n = 1, 2, 3, \dots \quad (9)$$

which implies that, for $\lambda = \lambda_0$, the output signal of the readout is at a maximum of interference. Under these circumstances, as the wavelength of the laser oscillates around λ_0, the readout signal does not contain any component oscillating at frequency ω:

$$W(t) \propto 1 + 0 \times \frac{\delta\lambda}{\lambda_0} \cos(\omega t) + O\left(x^2 \right) \quad (10)$$

From this example, it is clear that, by modulating the wavelength of the readout at frequency ω, one can distinguish maxima (or, equivalently, minima) of interference from quadrature points by measuring the component of the readout output signal that oscillates at frequency ω. To maintain the deflection of the cantilever constant, one can thus mount the probe on a piezoelectric stage that, driven by a high-gain negative feedback loop fed with a signal proportional to the ω component of the readout system, keeps the latter equal to zero.

Interestingly, to move from one maximum (or minimum) of interference to the next one, one needs to deflect the cantilever of an exact amount $\delta d = \lambda_0/2$. Measuring the change of weight registered by the balance as the cantilever moves through a series of maxima (or minima) of interference, it is then possible to obtain a calibration of the spring constant of the cantilever on the basis of only two parameters: the weights
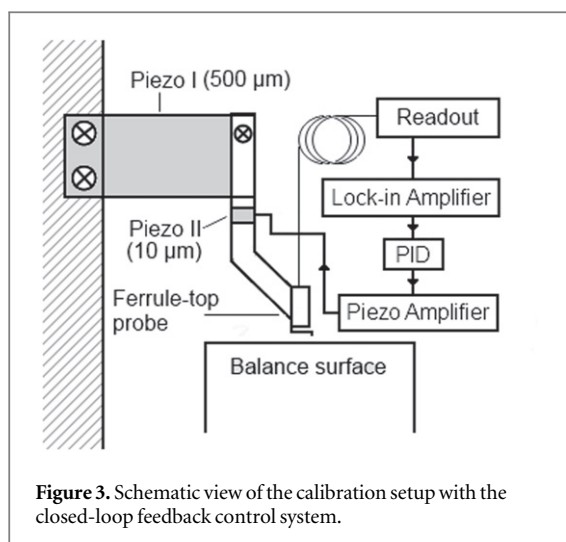
Figure 3. Schematic view of the calibration setup with the closed-loop feedback control system.

measured by the balance and the wavelength of the laser (λ_0).

2.4. Calibration method: experimental setup

Figure 3 shows a schematic view of the experimental setup used to demonstrate our calibration method.

The ferrule-top probe is connected to a commercial interferometer (OP1550, Optics11), which is equipped with a tunable infrared laser. The wavelength of the laser is internally controlled with 10 pm accuracy, and can be swept by driving the injection current with a sinusoidal signal. For our experiment, we used a central wavelength of 1531 nm, modulated at 10 kHz with a modulation amplitude of 0.5 mA, corresponding to a modulation of approximately 50–100 pm.

The probe is mounted on a large stroke (500 μm) piezoelectric translator (Piezo I in figure 3, P-603.5S1, PI GmbH) driven, in open loop, by a 5 nm resolution servo-controller (E-665.SR, PI GmbH). The holder contains a second piezoelectric translator (Piezo II in figure 3, 10 μm stroke, Thorlabs GmbH), which is operated in closed loop via a strain gauge system. For a controlled force measurement we make use of an analytical self calibration balance (MSE125P-100-DU, Sartorius AG) that has a readability of 15 μg (or force resolution of 150 nN) with an integration time of $\approx$ 6 s. To reduce vibrations and airflow, the setup is built within draft shields and is mounted on a passive anti-vibration stage (Nexus, Thorlabs GmbH).

The position of the cantilever is carefully controlled by means of a negative feedback circuit (gain = 19.8 dB, τ = 90 ms). This circuit is driven by a lock-in amplifier (SR830, Stanford Research Systems), which is locked at frequency ω. The time constant of the lock-in amplifier is set to 30 ms. A proportional-integral-derivative controller, driven by the lock-in amplifier, is connected to the 10 μm stroke piezoelectric translator to adjust the bending of the cantilever such that the output of the lock-in amplifier, at

frequency ω, is set to zero, corresponding to a maximum (or minimum) of interference.

2.5. Experimental procedure

To demonstrate the working principle, we have calibrated the ferrule-top cantilever described in the previous section according to the following procedure.

The ferrule-top probe is positioned, within 2 μm above the weighing pan of the balance, by means of the large-stroke z-translator (Piezo I). The loop is then closed, causing the second piezoelectric translator to scan down, bring the probe in contact with the pan of the weighing scale, and compress the cantilever until it encounters the first maximum of interference. The weight measured while the applied force is locked to this set value is the first measurement point of our experiment.

Starting from this maximum of interference, then, we apply, in closed loop, a step of approximately $\frac{1}{2}\lambda_0$ to Piezo I with a stroke significantly faster than the reaction time of the feedback (τ = 90 ms). This procedure allows us to move to the next maximum of interference, thereby increasing the cantilever deflection. The step size of the z-translator does not have to be exactly $\frac{1}{2}\lambda_0$: since the loop is still closed, the small-stroke piezoelectric translator adjusts the bending of the cantilever in such a way that the signal is locked to the next maximum, corresponding to an additional deflection of exactly $\frac{1}{2}\lambda_0$. Using this method discrete indentation steps of $n \times \frac{1}{2}\lambda_0$ are possible (with n = 1, 2, 3, ...), with a resolution corresponding to that of the laser wavelength (10 pm).

To calibrate the cantilever described in section 2.1, we repeated the calibration procedure explained above for nine times. Before each run, we calibrated the weighing scale using its internal calibration procedure. In each run, we measured the weight indicated by the scale for 20 steps of $\frac{1}{2}\lambda_0$ (λ_0= 1551 nm), resulting in a maximum cantilever deflection of around 16 μm, and then calculated the spring constant of the cantilever from the linear fit of the force-bending curve.

To illustrate the effect of the feedback loop on noise reduction, we also repeated a set of four runs with the feedback loop disabled.

3. Results and discussion

Figure 4(a) reports a typical force-bending curve obtained with the feedback loop method. A linear response is observed over the entire deflection range. Fitting each of the nine force-bending curve with a first order linear regression, and calculating the weighted average of the slope, one obtains a value for the spring constant of the cantilever equal to 1.1627 ± 0.0047 N m^{-1}. Figure 4(b) further shows the distribution of the residuals of the fits, which are indeed spread according to a Gaussian distribution. Performing a *t*-
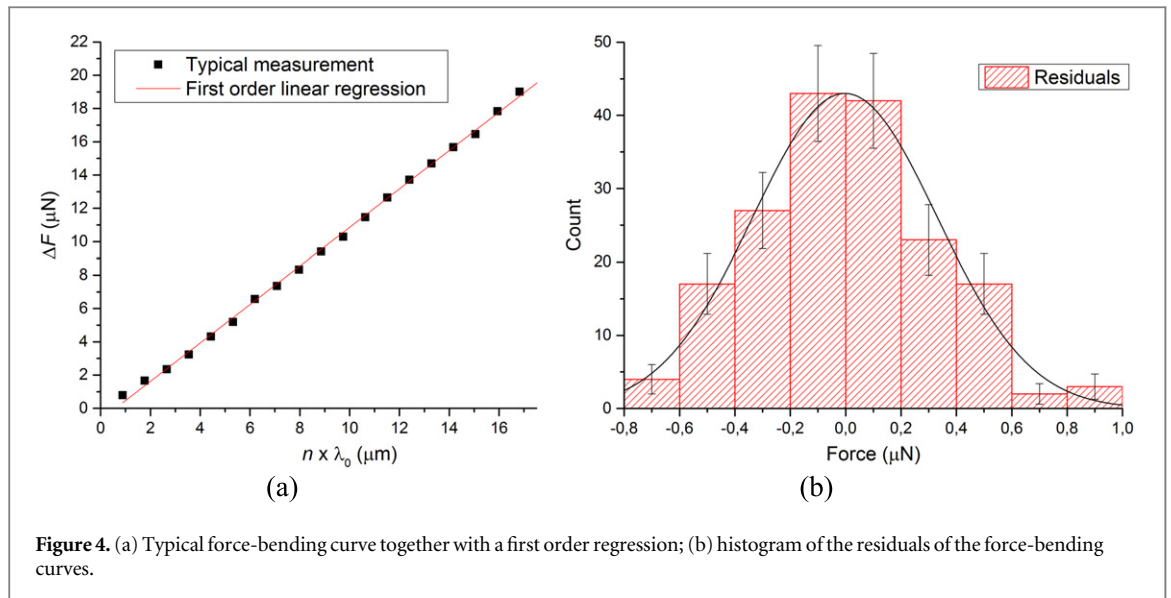
Figure 4. (a) Typical force-bending curve together with a first order regression; (b) histogram of the residuals of the force-bending curves.
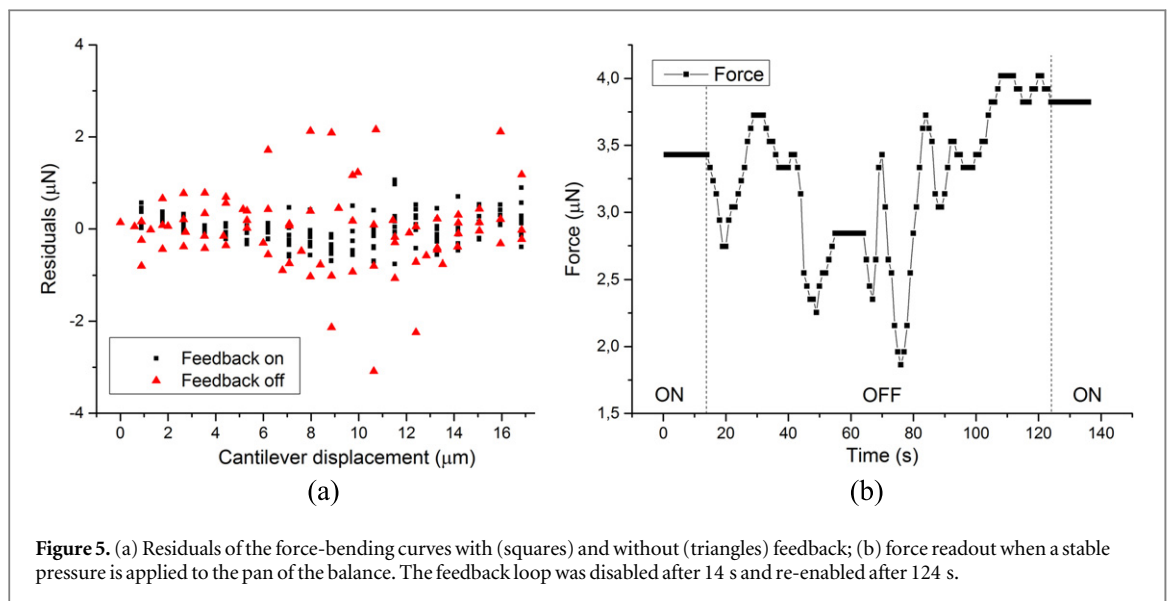

Figure 5. (a) Residuals of the force-bending curves with (squares) and without (triangles) feedback; (b) force readout when a stable pressure is applied to the pan of the balance. The feedback loop was disabled after 14 s and re-enabled after 124 s.

test on these data, one can show that the mean of the residuals does not significantly differ from zero ($p \ll 0.001$). Therefore it can be concluded that the linear regressions correlate very well with the obtained datasets.

To demonstrate the added value of the high-gain feedback loop, in figure 5(a) we compare the residuals of the force-bending curves obtained with our method with those obtained from the data collected in the 4 runs without feedback. It is clear that our method is indeed capable of reducing the error significantly. Figure 5(b) further shows the effect of the feedback loop when a constant pressure is applied to the pan of the balance. One can observe that, as soon as the feedback loop is disabled, the readout signal becomes much more noisy.

Concerning the systematic error, it is important to stress once again that our method completely eliminates the calibration of the piezoelectric transducer and significantly reduces the effects of mechanical

drifts. The changes in the bending of the cantilever, in fact, are multiples of the wavelength of the laser used in the interferometer, which, in our case, is known with an accuracy of ten parts per million, and is thus completely negligible. The main source of systematic error is the one introduced by the weighing scale, which is certified for 15 μg. A systematic error of 15 μg on the first and the last point of figure 4(a) would give rise to a systematic error on the spring constant of 0.0088 N m^{-1} ($\triangle k = \frac{\text{readability}}{\left(\frac{n\lambda}{2}\right)}$). Therefore, assuming that, after internal calibration, the systematic error of the balance is equal to its readability, we can conclude that the spring constant of the cantilever is equal to:

$$k = 1.1627 \pm 0.0047 \,(\text{stat})$$
$$\pm \, 0.0088 \,(\text{syst})\, \text{N m}^{-1}. \qquad (11)$$

Substituting the weighting scale with one with 100 ng readability (e.g., MSA2.7S-000-DF, Sartorius AG),

one could reduce the systematic error even further down to $\simeq 100\,\mu\,\mathrm{N\,m}^{-1}$.

It is important to stress that the calibration method presented here already accounts for the fact that the fiber is not aligned with the end of the cantilever, where the sphere enters in contact with the pan. When, after calibration, the transducer will be used in practical applications, in fact, the only information that the user will be able to obtain is the displacement of the cantilever at the point where the fiber is. Multiplying that number times the number indicated in equation (11), the user will now know exactly the magnitude of the force applied on the sphere at the end of the cantilever, which is the information that the force transducer is indeed supposed to give.

4. Conclusions

We have introduced an improved method for the calibration of force transducers with interferometric readout. This method relies on the application of a constant pressure by the sensor on an analytical balance using a negative feedback loop. The loop allows one to keep the displacement of the transducer stable over time and to simultaneously measure the displacement of the transducer as a multiple of the wavelength of the laser in the readout. By using this feedback loop, our calibration method is able to offer calibrations according to metrical standards. The key parameters, displacement and weight, are measured with an accuracy of 10 pm and 15 μg, respectively. Other advantages over the well-known calibration methods are high throughput and ease of use. The method presented is non-destructive (as long as the contact point of the transducer does not damage when a force is applied to it), reproducible, and universal, and can therefore pave the way for the use of more complex cantilever devices in the future.

Disclosures

D Iannuzzi is co-founder and shareholder of Optics11.

Acknowledgments

References

[1] García R and Pérez R 2002 *Surf. Sci. Rep.* **47** 197–301
[2] Butt H J, Cappella B and Kappl M 2005 *Surf. Sci. Rep.* **59** 1–152
[3] Burnham N A, Chen X, Hodges C S, Matei G A, Thoreson E J, Roberts C J, Davies M C and Tendler S J B 2003 *Nanotechnology* **14** 1
[4] Sader J E 1998 *J. Appl. Phys.* **84** 1089–7550
[5] Neumeister J M and Ducker W A 1994 *Rev. Sci. Instrum.* **65** 2527–31
[6] Clifford C A and Seah M P 2005 *Nanotechnology* **16** 1666
[7] Sader J E, Sanelli J A, Adamson B D, Monty J P, Wei X, Crawford S A, Friend J R, Marusic I, Mulvaney P and Bieske E J 2012 *Rev. Sci. Instrum.* **83** 103705
[8] Lübbe J, Doering L and Reichling M 2012 *Meas. Sci. Technol.* **23** 045401
[9] Cole D G 2008 *Meas. Sci. Technol.* **19** 125101
[10] Cleveland J P, Manne S, Bocek D and Hansma P K 1993 *Rev. Sci. Instrum.* **64** 403–5
[11] Sader J E, Larson I, Mulvaney P and White L R 1995 *Rev. Sci. Instrum.* **66** 3789–98
[12] Cook S M, Schäffer T E, Chynoweth K M, Wigton M, Simmonds R W and Lang K M 2006 *Nanotechnology* **17** 2135
[13] Palacio M L B and Bhushan B 2010 *Crit. Rev. Solid State Mater. Sci.* **35** 73–104
[14] te Riet J *et al* 2011 *Ultramicroscopy* **111** 1659–69
[15] Berger J, Švec M, Müller M, Ledinský M, Fejfar A, Jelínek P and Majzik Z 2013 *Beilstein J. Nanotechnology* **4** 1–9
[16] Cumpson P J and Hedley J 2003 *Nanotechnology* **14** 1279
[17] Clifford C A and Seah M P 2009 *Meas. Sci. Technol.* **20** 125501
[18] Gao S and Brand U 2014 *Meas. Sci. Technol.* **25** 044014
[19] Doering L, Peiner E, Nesterov V and Brand U 2006 *Proc. Nanoscale Calibration Standards and Methods: Dimensional and Related Measurements in the Micro- and Nanometer Range* pp 157–70 ch 12
[20] Rugar D, Mamin H and Guethner P 1989 *Appl. Phys. Lett.* **55** 2588–90
[21] Rasool H I, Wilkinson P R, Stieg A Z and Gimzewski J K 2010 *Rev. Sci. Instrum.* **81** 023703
[22] Morita K, Sugimoto Y, Sasagawa Y, Abe M and Morita S 2010 *Nanotechnology* **21** 305704
[23] Iannuzzi D *et al* 2007 *Meas. Sci. Technol.* **18** 3247
[24] Gruca G, Man S D, Slaman M, Rector J H and Iannuzzi D 2010 *Meas. Sci. Technol.* **21** 094033
[25] Gruca G, Chavan D, Rector J, Heeck K and Iannuzzi D 2013 *Sensors Actuators* A **190** 77–83
[26] Chavan D, Watering T C V D, Gruca G, Rector J H, Heeck K, Slaman M and Iannuzzi D 2012 *Rev. Sci. Instrum.* **83** 115110
[27] Chavan D, Gruca G, de Man S, Slaman M, Rector J H, Heeck K and Iannuzzi D 2010 *Rev. Sci. Instrum.* **81** 123702
[28] Chavan D, Mo J, de Groot M, Meijering A, De Boer J F and Iannuzzi D 2013 *Opt. Lett.* **38** 1476–8
[29] van Hoorn C H, Chavan D C, Tiribilli B, Margheri G, Mank A J G, Ariese F and Iannuzzi D 2014 *Opt. Lett.* **39** 212880
[30] Hooke R 1678 *Lectures de Potentia Restitutiva, or of Spring Explaining the Power of Springing Bodies* (London: J. Martyn)